Anion binding based on Hg_3-anticrowns as multidentate Lewis acidic hosts

Oliver Loveday,[a] Jesús Jover[a] and Jorge Echeverría[b]*

a) Secció de Química Inorgànica, Departament de Química Inorgànica i Orgànica and Institut de Química Teòrica i Computacional (IQTC-UB), Universitat de Barcelona, Martí i Franquès 1-11, 08028, Barcelona (Spain).

b) Departamento de Química Inorgánica, Instituto de Síntesis Química y Catálisis Homogénea (ISQCH), CSIC-Universidad de Zaragoza, Pedro Cerbuna 12, 50009 Zaragoza (Spain).

e-mail: jorge.echeverria@unizar.es

Abstract

We present herein a combined structural and computational analysis of the anion binding capabilities of perfluorinated polymercuramacrocycles. The Cambridge Structural Database (CSD) has been explored to find the coordination preference of these cyclic systems towards specific Lewis bases, both anionic and neutral. Interaction energies with different electron rich species have been computed and further decomposed into chemically meaningful terms by means of energy decomposition analysis. Furthermore, we have investigated, by means of NRT and NBO analyses how the orbitals involved in the interaction are key in determining the final geometry of the adduct. Finally, a generalization of the findings in terms of molecular orbital theory has allowed us to understand the formation of the pseudo-octahedral second coordination sphere in linear Hg(II) complexes.

INTRODUCTION

The design and synthesis of chemical systems that efficiently recognize and capture anions have attracted increasing attention during the last decades.[1] Anion binding is based on the establishment of noncovalent interactions, *e.g.*. hydrogen and halogen bonds, between the anion and the molecular host.[2] Several families of compounds have been used to capture different types of anionic systems, as for instance cryptands,[3] cucurbiturils[4, 5] or calixarenes.[6, 7] Recently, transition metal-based anion receptors have been investigated as promising anion capturers.[8] These systems bind anions via their ligands or directly through the metal center by means of metal···anion interactions. Among the latter, polymetallic macrocycles make use of simultaneous interactions with multiple metal centers to improve the anion binding capacity. Recently, the capture of halide anions by cyclic $(Py\text{-}M)_3$ (M = Cu, Ag, Au) systems has been computationally studied.[9]

Perfluorinated polymercuramacrocycles are a family of compounds with enhanced electrophilicity due to the presence of several Lewis acid centres that can act coordinatively to bind a wide range of anions. Moreover, the presence of peripheric fluorine atom increases the electron density depletion in the central region of the molecule. Polymercuramacrocycles have been generally termed anticrowns since they can be seen as the electron-deficient equivalents of crown ethers.[10] Here, we narrow our focus on perfluoro-*o*-phenylenemercury ($(o\text{-}C_6F_4Hg)_3$; see Scheme 1). Ever since being first synthesized in the 1960s,[11] the anion binding capabilities of this compound have been extensively investigated.[12] The high degree of preorganization along with the simultaneous action of three Lewis acidic centres make ($(o\text{-}C_6F_4Hg)_3$ a versatile and efficient anion capturer.

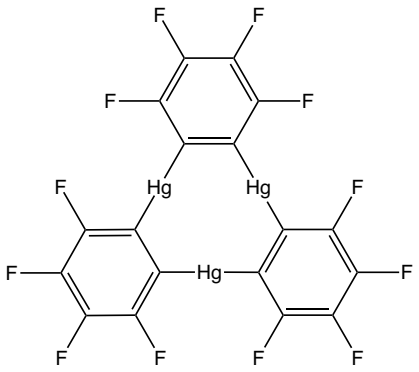

Scheme 1. Chemical structure of perfluoro-*o*-phenylenemercury ($(o\text{-}C_6F_4Hg)_3$).

Herein, we intend to study, by means of computational tools, the interaction of this anticrown with several anionic species, but also with neutral electron-rich species that are often used as solvents. We will analyse the nature of the interaction with different Lewis bases (LB) and how electrostatics and, in particular, orbital interactions determine the final geometry and stability of the adduct.

RESULTS AND DISCUSSION

Experimental crystal structures

The molecular electrostatic potential (MEP) of the (*o*-$C_6F_4Hg)_3$ molecule clearly displays a region of electron density depletion ($V_{s,max}$ = +60.3 kcal/mol) located at the centre of the triangle formed by the three Hg atoms (Fig. 1). This electrophilic region is significantly exposed due to the planarity of the molecule and, thus, able to be reached by electron-rich species, both anionic and neutral. In fact, there are many examples in the Cambridge Crystallographic Database (CSD) in which a LB interacts with the electron-depleted region involving three Hg···LB distances shorter than the sum of the van der Waals radii.[13] Here, the (*o*-$C_6F_4Hg)_3$ molecule behaves as a three-dentate Lewis acid via its three Hg(II) centres. On the other hand, we have observed a marked variability in the nature of the interacting LB, including both neutral and anionic species such as benzene (ABELUO),[14] naphthalene (MOXMIV),[15] triphenylene (MOXMOB),[15] corannulene (IXOBAZ),[16] *closo*-dodecaborate (ACEREF),[17] dimethylsulfoxide (CAMFOM),[18] methyl parathion (CEJNUB),[19] ferrocene (FANNUE)[20] and nickelocene (FANPAM)[20] *via* their Cp ligands, nitrate (HIMHUI),[21] nitrobenzene via the O atoms (REWZID),[22] dimethylsulfide (UKUQEW),[23] carbon disulfide (PAGLIT),[24] coordinated pentaphosphole (JOVHOT)[25] and pentarsolyl (JOVVOH)[25] and polyynes through their triple bonds (JEGLEN).[26] In Fig. 2, two selected examples are shown in which the Lewis base is dimethylketone and chloride (MUPXAW[27] and YOLCAG,[28] respectively).

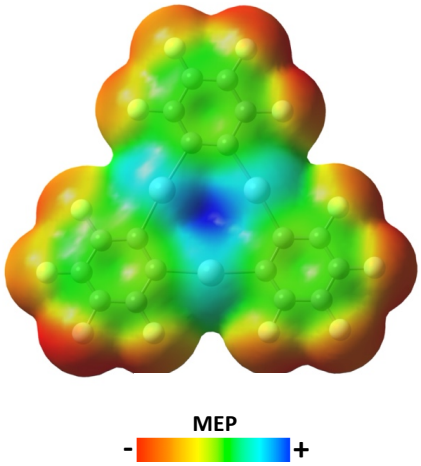

Figure 1. Molecular electrostatic potential map on the s = 0.001 isosurface of (*o*-$C_6F_4Hg)_3$.

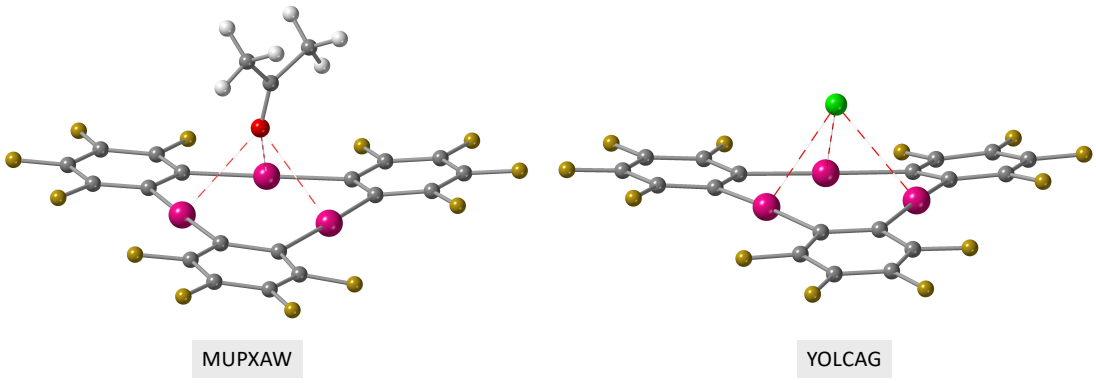

Figure 2. Short Hg···O and Hg···Cl contacts (red dashed lines) found in the crystal structures of {[(*o*-$C_6F_4Hg)_3$](Me-CO-Me)$_3$} (MUPXAW)[27] and [$(CH_2)_{10}(NH_2)_2(NH)_2$]{[(*o*-$C_6F_4Hg)_3$]$Cl_2$} (YOLCAG),[28] respectively.

It is worth noting the tendency of halide anions in crystalline phases to bind Hg centers of the Hg_3-anticrown instead of the corresponding counter-cations. For instance, in the crystal structure of [PPh_4]{[(*o*-$C_6F_4Hg)_3$]$_2$F}, the fluoride anion is placed between two Hg_3-anticrowns forming a sandwich-like structure, while the large tetraphenylphosphonium interacts with the ensemble through C-H/π and C-H···F-C interactions (Fig. 3).

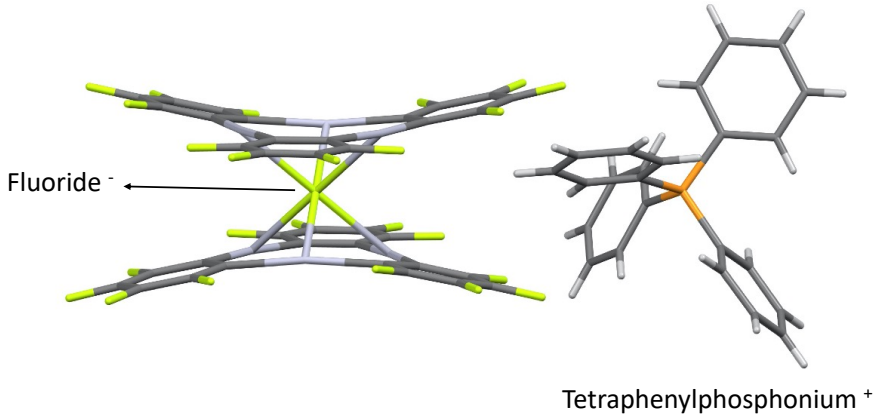

Figure 3. Crystal structure of $[PPh_4]\{[(o\text{-}C_6F_4Hg)_3]_2F\}$ (UTOZEK).[29]

Geometry of the adducts and interaction energies

We have performed a computational study of the interaction geometries and strength of several models composed of $(o\text{-}C_6F_4Hg)_3$ and different Lewis bases, both charged and neutral. The main results, which are compared to experimental structures when available, are presented in Table 1. In general, the DFT results fairly reproduce the geometries observed in crystal structures. For monoatomic anions, DLPNO-CCSD(T) interaction energies are considerably high and depend on the size of the anion, being maximum for hydride (-96.9 kcal/mol) and minimum for iodide (-48.8 kcal/mol). It is interesting to note that the interaction energies calculated for anions show a nice linear correlation ($R^2 = 0.97$) with the degree of penetration between X and Hg atoms[30] (see Fig. S1 in the Supp. Info.) On the other hand, for neutral LBs the strength of the interaction diminishes significantly, ranging from -9.7 kcal/mol for water to -16.0 kcal/mol for acetone. These results are a good indicator of the capability of Hg_3-anticrowns to be exploited as anion capturers. If we look at the equilibrium geometries, there also are some differences between anionic and some of the neutral LBs. While the three Hg···LB distances for anions, acetone and acetonitrile are practically the same, in the case of dimethyl ether one of the computed Hg···O contacts is significantly shorter than the other two (2.949 and 3.438/3.4507 Å, respectively), which could be attributed to the establishment of CH/π interactions between a methyl group and one of the aromatic rings of the anticrown. For water, however, there are two practically identical distances (3.067 Å) and a significantly longer one (3.403 Å). Since such geometry cannot be related with any secondary noncovalent interaction between the Hg_3 anticrown and the Lewis base, it must be due to some particular feature of the water-Hg interaction.

Table 1. Distances between mercury atoms and the donor atom of the Lewis base (LB) calculated after full geometry optimization (B3LYP-D3BJ/def2-TZVPD) of the adducts formed by (*o*-$C_6F_4Hg)_3$ and the different LBs. Experimental distance values are given for comparison when available. Interaction energies (ΔE_{int}) are obtained at the DLPNO-CCSD(T)/def2-TZVPD level on the DFT optimized geometries.

LB	LB···Hg exp. (Å)	Refcode	LB···Hg calc. (Å)	ΔE_{int} (kcal/mol)
H^-	- - -	-	2.126 2.126 2.126	-96.9
F^-	2.620 2.614 2.647	UTOZEK[29]	2.470 2.471 2.471	-80.8
Cl^-	2.994 3.005 3.023	YOLCAG[28]	2.944 2.944 2.943	-58.2
Br^-	- - -	-	3.098 3.098 3.098	-53.8
I^-	3.261 3.321 3.389	UTOMAT[29]	3.298 3.298 3.298	-48.8
H_2O	2.821 2.928 3.136	OYAPUA[31]	3.067 3.067 3.403	-9.7
Me-O-Me	- - -	-	2.949 3.438 3.457	-13.4
Me-CO-Me	2.815 2.858 2.906	MUPXAW[27]	2.974 3.021 3.027	-14.4
Me-CN	2.930 2.932 2.989	WOSFAL[32]	3.113 3.113 3.114	-16.0

Although this behavior is also observed in the crystal structure of [(*o*-$C_6F_4Hg)_3$] dihydrate (OYAPUA),[31] we wanted to be sure that the out-of-the-centre displacement from our calculations is not just the consequence of a flat potential energy surface (PES) in the central region of the Hg_3 system. To do so, several starting geometries were used in the optimizations, leading in all cases to the same equilibrium geometry, which was confirmed to be a real minimum of the PES by computation of the corresponding vibrational frequencies. Furthermore, we defined an angle α between the donor atom of the LB, the centroid of the Hg_3 system and one of the Hg atoms (Fig. 4 inset) and we

searched the CSD for short LB···Hg_3 contacts for different families of LBs. The results representing the average values of the smallest angle α are summarized in Fig. 4. It can be seen that, while for halides the angle α is very close to 90º, it diminishes (i.e. moves off the Hg_3 centre) for nitriles and ketones, being the decrease more pronounced when the donor is a ether-like sp^3-oxygen atom (averaged smallest angle α = 84.5º). This confirms the different behaviour, both experimental and computational, of water and ethers with respect to the other studied LBs.

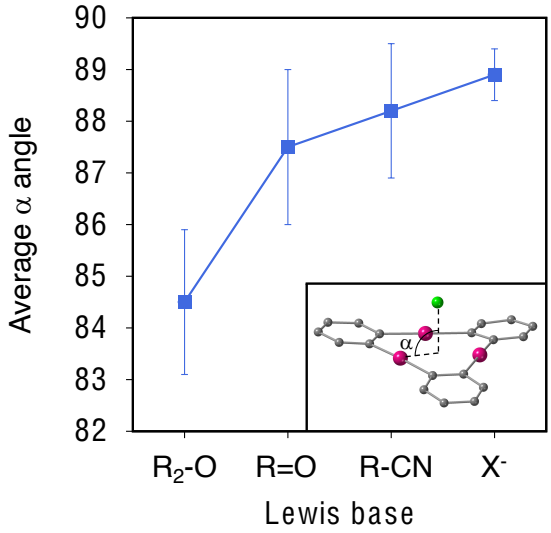

Figure 4. Variation of the averaged smallest Hg-centroid-LB (α) angle as a function of the nature of the donor atom.

Energy decomposition analysis (EDA)

To gain further insight into the nature of the interactions, we have carried out an Energy Decomposition Analysis (EDA) of the model systems in Table 1. We applied the ALMO-EDA scheme that decomposes the interaction energy into terms that are chemically meaningful ($\Delta E_{INT} = \Delta E_{FRZ} + \Delta E_{POL} + \Delta E_{CT}$). The ΔE_{FRZ} term represents the energy changes associated with bringing together two fragments that were infinitely separated without any relaxation of their MOs. On the other hand, ΔE_{POL} and ΔE_{CT} terms account for the energy stabilization due to *intrafragment* and *interfragment* relaxation of the Mos, respectively. Representative EDA results are shown in Table 2 (see Table S1 in the Supp. Info. for further decomposition of the Frozen term).

Table 2. Energy Decomposition Analysis (EDA) calculated at the B3LYP-D3BJ/def2-TZVPD level for the adducts formed by (*o*-$C_6F_4Hg)_3$ and the different LBs. All energies in kcal/mol.

LB	ΔE_{FRZ}	ΔE_{POL}	ΔE_{CT}	ΔE_{INT}
H^-				
F^-	-11.3	-51.3	-18.1	-80.8
Cl^-	-7.1	-31.9	-21.8	-60.8
Br^-	-6.2	-28.8	-21.9	-56.9
I^-	-4.1	-25.2	-23.8	-53.2
H_2O	-4.5	-2.1	-2.0	-8.6
Me-O-Me	-6.9	-2.8	-2.9	-12.5
Me-CO-Me	-7.0	-4.3	-3.2	-14.5
Me-CN	-5.6	-3.6	-3.0	-12.2

A molecular orbital approach

It seems now clear that the trend in the equilibrium geometries observed both computationally and experimentally cannot be explained by using MEP maps as the only predictors. Previous reports have also shown the incapability of MEP maps to rationalize interactions in which repulsive Coulombic forces (predicted by MEPs) are overcome by dispersion and/or orbital charge transfer (both invisible for MEPs).[33-36] In the light of this, and according to our EDA results above, we wondered if the particular behavior of water towards Hg_3-anticrowns can be the result of specific orbital interactions. In order to unveil any charge transfer process between the Lewis acidic and basic species we need first to establish the mercury-centred molecular orbitals that are able to delocalize electron density from the LBs lone pairs.

In Fig. 5, we show a qualitative molecular orbital diagram for a simple dicoordinated Hg(II) complex, namely $HgCl_2$. It is known that the 6*s* orbital in mercury, as in other heavy metals, is contracted due to relativistic effects, which makes difficult its hybridization with empty 6*p* orbitals because of the large energy difference. In fact, the predominance of linear dicoordination in Hg(II) complexes can be explained by the absence of *s*-*p* hybridization. A consequence of this is the presence of two degenerate

antibonding π* orbitals (LUMO+1 in LUMO+2 in Fig.5) that, *a priori*, can act as charge transfer acceptors from a LB.

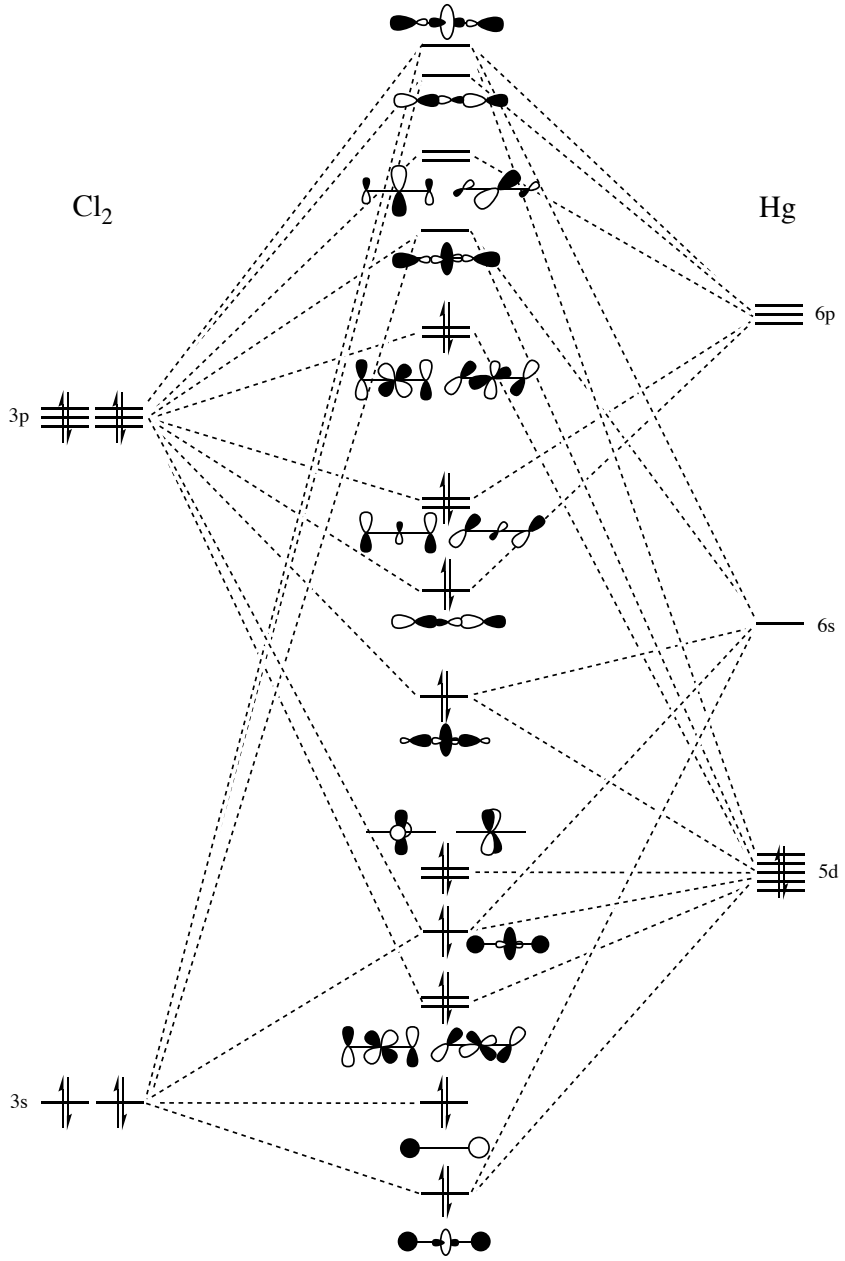

Figure 5. Qualitative molecular orbitals diagram of the $HgCl_2$ molecule.

The presence of a set of two empty *p* orbitals at each mercury cation should, in fact, allow its interaction with up to four extra LBs, yielding a linear geometry (coordination number = 2) at the typical coordination bonds distances and *k* (*k* = 1 – 4) extra ligands at longer distances, but shorter than the vdW radii sum (Fig 6a). This explains the persistence among Hg(II) complexes of geometries such as T-shaped (*k* = 1) or octahedral (*k* = 4). The idea of a double coordination sphere in Hg(II) complexes, comprising a characteristic and effective coordination (2 + *k*), is not new since it was

proposed by Grdenić in 1965.[37] Early theoretical work by Kaupp *et al*. further investigated this particular behaviour in HgX_2 dimers (X = F, Cl, Br, I, H).[38, 39] If we look at Hg_3-anticrowns, there are several examples in the CSD with a linear Hg(II) centre in $(o\text{-}C_6F_4Hg)_3$ interacting with up to four extra LBs. For instance, in the crystal structure of IHINIX,[40] one of the dicoordinated mercury centres interacts with four tetrahydrofurane molecules (Fig. 6b), resulting in a pseudo-octahedral coordination geometry with the four extra LBs forming an slightly distorted square-planar structure (Continuous Shape Measure $S_{(SP\text{-}4)} = 2.53$). This clearly indicates that the set of two empty *p* orbitals of Hg dictates the final geometry of these 2 + *k* coordination complexes. In fact, the formation of a reverse sandwich-like structure, with two LBs (each binding the three mercury atoms) above and below the anticrown, is a recurrent pattern in the CSD.

The interaction of Hg_3-anticrowns and electron rich species has been extensively investigated by the Gabbaï group. They rationalized such interactions in terms of both electrostatics and orbital charge transfer,[41] proposing for the first time the participation of mercury 6*p* orbitals as electron density acceptors.[14] Moreover, a nice example of how orbital interactions can determine the final geometry of an adduct was reported in 2003 by Tsunoda and Gabbaï.[23] They presented crystallographic evidence of the interaction of two $(o\text{-}C_6F_4Hg)_3$ with dimethyl sulfide involving a Hg_3 centroid−S−Hg_3 centroid angle of 135.6°, which is the result of the interaction of only one of the sulfur lone pairs with the two sets of three mercury *p* orbitals above and below the dimethyl sulfide molecule.

In previous reports, the interaction of linear group 12 complexes with extra ligands has been theoretically studied within the π-hole bonding framework.[42, 43] On the other hand, in molecular orbital theory, the effective coordination sphere can be rationalized in terms of the Rundle-Pimentel model in which two 3c-4e bonds are formed (Fig. 6c). The interaction of the two empty p orbitals of the MX_2 framework with four lone pairs (4Y) from the LBs forms two bonding, two non-bonding and two antibonding molecular orbitals that leads to the MX_2Y_4 complex, yielding a net energy stabilization of the system, which allows understanding the generalized presence of Hg(II) complexes with 2 + *k* coordination in the solid state.

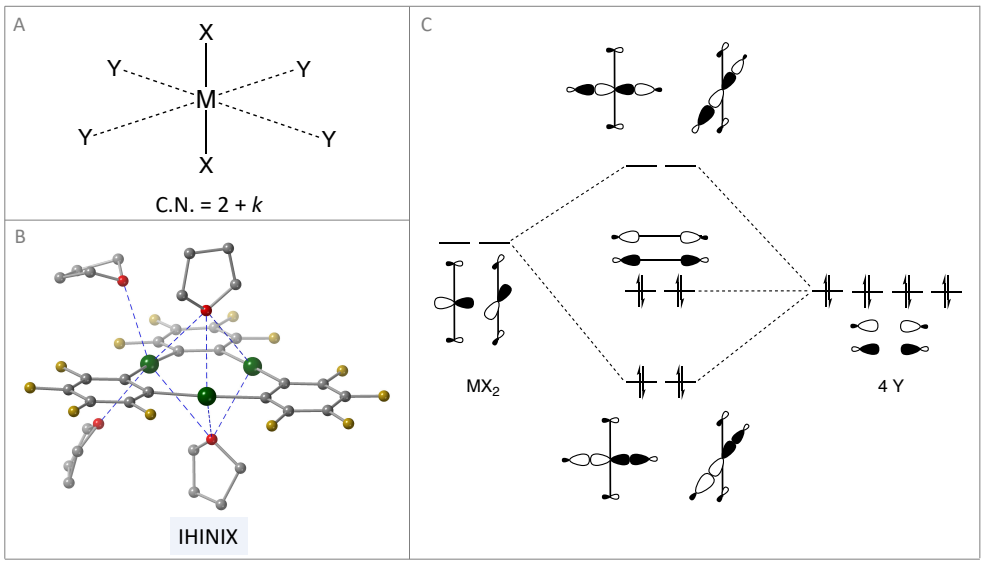

Figure 6. a) Characteristic and effective coordination spheres in pseudo-octahedral HgX_2Y_4 complexes, (b) example of pseudo-octahedral coordination in Hg_3-anticrowns found in the crystal structure of IHINIX[40] and (c) molecular orbitals diagram for the formation of the effective coordination sphere in MX_2 cores.

Natural Resonance Theory (NRT) and Natural Bond Orbital (NBO) analyses

As previously pointed out by Coulson[44] and then by Weinhold,[45] the electron density distribution associated with the 3c-4e Rundle-Pimentel model for linear systems can be equally described by the resonating ω-bonding model within the natural bond orbital (NBO) formalism.[46] Accordingly, we have applied the natural resonance theory (NRT)[47] to the simple $HgCl_2$ complex studied above. NRT calculations have disclosed that the system is better described as a resonance 3c/4e triad Cl: Hg–C ⇔ C–Hg :Cl arising from hyperconjugation interactions, with resonance weightings for each of the two resonance structures of 50%, and a natural atomic valence for Hg of 1.0. This bonding picture is in good agreement with previous NRT analyses in related transition metal systems.[48, 49] Further exploratory NRT calculations on the F_5C_6-Hg-C_6F_5 complex, closer to the Hg_3-anticrown, disclose a more complex bonding scenario with multiple contributing resonant structures, with those that involve C: Hg–C ⇔ C–Hg :C resonance accounting for up to 60% of the resonant weighting.

Keeping this in mind, we have next carried out a comprehensive NBO analysis of all the studied adducts. The results are presented in Table 3. Remarkably, in all cases, the

acceptor orbitals are $\sigma^*_{Hg\text{-}C}$ orbitals since the NBO scheme considers the C-Hg-C moieties as 3c/4e hyperbonds as in the Hg-Cl case described above. The largest second order perturbation energies ($E^{(2)}$) are found for hydride, which is the LB with the highest degree of penetration among all studied adducts (*p*H-Hg = 75.4 %). For halides, the charge transferred is the same towards each of the three Hg centres and it does not vary significantly as we descend the group, accounting for a total $E^{(2)}$ of 20.1 kcal/mol for iodide. For LBs with oxygen as the donor atom (*i.e.* water, dimethyl ether and acetone), more differences are found between the three Hg centres. In the case of acetone, the charge transfer is similar towards the three metal centres. For dimethyl ether, one metal centre accepts 77.5% of the total amount of charge transfer while the other 22.5% is equally distributed between the other two Hg centres. Finally, in the case of water, there are two Hg centres that accumulate more than 80% of the total charge transfer (39.3 and 43.7%, respectively). When the LB is acetonitrile the donor orbital is an sp hybrid that delocalizes electron density into the σ antibonding orbital of each Hg cation (33.3% of the total CT to each Hg) and the total $E^{(2)}$ is one order of magnitude smaller than those calculated for halides. A comparative graphical summary of these processes can be seen in Fig. 7.

Table 3. Donor-acceptor orbital interactions and associated second order perturbation energies ($E^{(2)}$) obtained by means of NBO analysis for the adducts formed by $(o\text{-}C_6F_4Hg)_3$ and different LBs.

[a] The values of $E^{(2)}$ correspond to the sum of the electron transfer from each of the four lone pairs in each halide anion.

LB	Donor	Acceptor	$E^{(2)}$ (kcal/mol)
H^-	n_H (99% *s*)	$\sigma^*_{Hg1\text{-}C}$	25.23
		$\sigma^*_{Hg2\text{-}C}$	24.27
		$\sigma^*_{Hg3\text{-}C}$	24.65
F^-	n_F[a]	$\sigma^*_{Hg2\text{-}C}$	6.63
		$\sigma^*_{Hg3\text{-}C}$	6.57
		$\sigma^*_{Hg3\text{-}C}$	6.57
Cl^-	n_{Cl}	$\sigma^*_{Hg1\text{-}C}$	6.49
		$\sigma^*_{Hg2\text{-}C}$	6.55
		$\sigma^*_{Hg3\text{-}C}$	6.54
Br^-	n_{Br}	$\sigma^*_{Hg1\text{-}C}$	6.65
		$\sigma^*_{Hg2\text{-}C}$	6.65
		$\sigma^*_{Hg3\text{-}C}$	6.65

I^-	n_I	$\sigma^*_{Hg1\text{-}C}$	6.80
		$\sigma^*_{Hg2\text{-}C}$	6.78
		$\sigma^*_{Hg3\text{-}C}$	6.79
H_2O	n_O (52% *s*; 48% *p*)	$\sigma^*_{Hg1\text{-}C}$	0.48
		$\sigma^*_{Hg2\text{-}C}$	0.55
		$\sigma^*_{Hg3\text{-}C}$	0.35
	n_O (99% p)	$\sigma^*_{Hg1\text{-}C}$	0.33
		$\sigma^*_{Hg2\text{-}C}$	0.35
Me-O-Me	n_O (45% *s*; 55% *p*)	$\sigma^*_{Hg1\text{-}C}$	0.10
		$\sigma^*_{Hg2\text{-}C}$	0.10
		$\sigma^*_{Hg3\text{-}C}$	1.01
	n_O (99% *p*)	$\sigma^*_{Hg1\text{-}C}$	0.08
		$\sigma^*_{Hg2\text{-}C}$	0.06
		$\sigma^*_{Hg3\text{-}C}$	0.16
Me-CO-Me	n_O (58% *s*; 42% *p*)	$\sigma^*_{Hg1\text{-}C}$	0.71
		$\sigma^*_{Hg2\text{-}C}$	0.41
		$\sigma^*_{Hg3\text{-}C}$	0.36
	n_O (99% *p*)	$\sigma^*_{Hg1\text{-}C}$	0.38
		$\sigma^*_{Hg2\text{-}C}$	0.44
		$\sigma^*_{Hg3\text{-}C}$	0.38
Me-CN	n_N (53% *s*; 47% *p*)	$\sigma^*_{Hg1\text{-}C}$	0.74
		$\sigma^*_{Hg2\text{-}C}$	0.76
		$\sigma^*_{Hg3\text{-}C}$	0.75

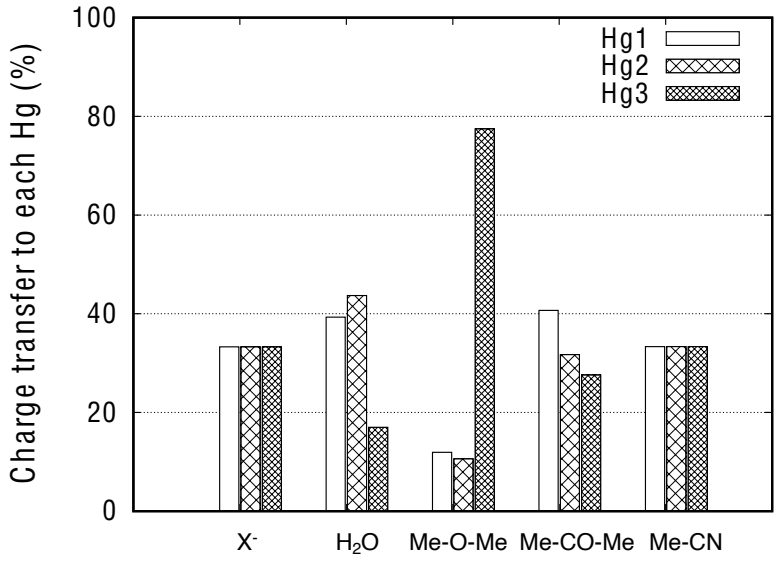

Figure 7. Amount of charge transfer (in percentage) to each of the three mercury centres for the different LBs.

The different behaviour of the studied LBs with respect to the charge transfer distribution between the three metal centres can be explained in terms of the shape and

size of the involved orbitals. We have mentioned before that the acceptor orbitals are empty σ antibonding Hg-C orbitals. On the other hand, the electron density donor orbitals involved vary in composition and number. In the case of O-donor LBs, there are two lone pairs involved as donors, one is an *sp* hybrid while the other one is a pure *p* orbital. We think that, in these cases, the presence of these *p* lone pairs determines the geometry of the adducts. For an optimum overlap of them with the acceptor orbitals, the LB must be closer to two mercury cations. This explains the larger out-of-centre displacement found, both experimentally (Fig. 4) and computationally (Table 1), for R_2O donors.

For halides, the four lone pair orbitals present some interesting features. There are two *p* lone pairs that remain non-hybridized (99.9% *p*) while the remaining *p* and the *s* lone pairs mix to different degrees to form two hybrids, $s^x p^y$ and $s^y p^x$. The degree of *sp* hybridization is maximum for F (x = 0.85, y = 0.15) and minimum for I (x = 0.95, y = 0.05). If we look back at the EDA analysis, while the charge transfer is practically the same for all halides and the changes in the Frozen term are small, the polarization term, associated with *intrafragment* reorganization of the MOs, significantly decreases when descending the group and shows a nice linear correlation with the *sp* hybridization degree seen in the NBO orbitals ($R^2 = 0.99$; see Fig. S2 in the Supp. Info.). Thus, we can conclude that the internal MOs relaxation, *i.e.* rehybridization, of the halide anions upon interaction is responsible for (1) the large interaction energies computed for halides and (2) the significant decrease in the interaction strength when descending the halogen group.

CONCLUSIONS

The performance of Hg_3-anticrowns, in particular ($(o\text{-}C_6F_4Hg)_3$, as anion capturers has been evaluated by means of structural and computational analyses. CSD searches have disclosed that these systems are able to bind a large range of electron rich species, including anionic and neutral LBs. The molecular electrostatic potential of the anticrown has clearly shown the Lewis acidic character of the central part of the molecule. We have calculated remarkably large interaction energies with monoatomic anions, showing less affinity for neutral species often used as solvents as, for instance, water or acetonitrile. Although the electrostatic analysis predicts the interaction of the LB with the centre of the anticrown, we have observed an unexpected out-of-centre displacement of the binding site for some Lewis bases, which we have been able to explain by means of an analysis of the orbitals involved in the interaction. Furthermore, a generalization of the findings in terms of molecular orbital theory and natural bond orbital has helped us to

understand the effective coordination sphere in linear mercury complexes. These results will be useful for the development of improved anion receptors based on polydentate macrocyclic systems and to further understand the peculiar coordination chemistry of d^{10} closed-shell heavy metals such as Hg(II) and Au(I).

COMPUTATIONAL METHODS

Structural searches were performed in the Cambridge Structural Database (CSD)[50] version 5.41 (November 2019) + 3 updates, allowing only crystal structures with 3D coordinates determined, with no errors and R factor smaller than 0.1. All electronic structure calculations were carried out with Gaussian16.[51] Based on previous benchmark studies on mercury complexes,[52] we employed the hybrid B3LYP functional with Grimme's empirical dispersion and Becke-Johnson dumping (B3LYP-D3BJ) and a triple quality def2-TZVPD basis sets for all atoms, including the corresponding relativistic pseudopotentials for heavy atoms. All systems in Table 1 were fully optimized and confirmed to be real minima of the corresponding potential energy surfaces by means of vibrational analysis. Interaction energies were calculated via the supermolecule approach (ΔE_{int} (AB) = $E_{AB} - (E_A + E_B)$) at the DLPNO-CCSD(T) level on the DFT-optimized systems without correction of the BSSE.[53] MEP maps were built with GaussView[54] on the 0.001 au isosurface. The interaction energies were decomposed into chemically meaningful terms ($\Delta E_{INT} = \Delta E_{FRZ} + \Delta E_{POL} + \Delta E_{CT}$) by means of the second generation ALMO-EDA procedure as implemented in QChem5[55] at the B3LYP-D3BJ level. The presence of pseudopotentials to describe heavy atoms forced us to apply the classical decomposition of the frozen energy ($\Delta E_{FRZ} = \Delta E_{Pauli}^{MOD} + \Delta E_{Elect}^{CLS} + \Delta E_{Disp}^{CLS}$). NRT and NBO analysis were done with the NBO7 program[56] on the optimized geometries. Molecular orbital diagrams are qualitative and based on the Khon-Sham orbitals calculated at the B3LYP level.

ASSOCIATED CONTENT

Supporting Information

Cartesian coordinates of all optimized systems.

Notes

The authors declare no competing financial interest.

ACKNOWLEDGEMNETS

This work was done thanks to project PID2019-109119GA-I00 and grant RYC-2017-22853 funded by MCIN/AEI /10.13039/501100011033 and by "ESF Investing in your future". J.E. is grateful to Gobierno de Aragón-ESF (Research Group E07_20R) for financial support. We thank Prof. Frank Weinhold for assistance with the NBO analysis.

REFERENCES

(1) Macreadie, L. K.; Gilchrist, A. M.; McNaughton, D. A.; Ryder, W. G.; Fares, M.; Gale, P. A., Progress in anion receptor chemistry. *Chem* **2022,** 8, 46-118.
(2) Chudzinski, M. G.; McClary, C. A.; Taylor, M. S., Anion Receptors Composed of Hydrogen- and Halogen-Bond Donor Groups: Modulating Selectivity With Combinations of Distinct Noncovalent Interactions. *Journal of the American Chemical Society* **2011,** 133, 10559-10567.
(3) Kang, S. O.; Llinares, J. M.; Day, V. W.; Bowman-James, K., Cryptand-like anion receptors. *Chem. Soc. Rev.* **2010,** 39, 3980-4003.
(4) Barrow, S. J.; Kasera, S.; Rowland, M. J.; del Barrio, J.; Scherman, O. A., Cucurbituril-Based Molecular Recognition. *Chem. Rev.* **2015,** 115, 12320-12406.
(5) Lagona, J.; Mukhopadhyay, P.; Chakrabarti, S.; Isaacs, L., The Cucurbit[n]uril Family. *Angew. Chem. Int. Ed.* **2005,** 44, 4844-4870.
(6) Matthews, S. E.; Beer, P. D., Calixarene-based Anion Receptors. *Supramol. Chem.* **2005,** 17, 411-435.
(7) Lhoták, P., Anion Receptors Based on Calixarenes. In *Anion Sensing: -/-*, Stibor, I., Ed. Springer Berlin Heidelberg: Berlin, Heidelberg, 2005; pp 65-95.
(8) Mercer, D. J.; Loeb, S. J., Metal-based anion receptors: an application of second-sphere coordination. *Chem. Soc. Rev.* **2010,** 39, 3612-3620.
(9) Alkorta, I.; Elguero, J.; Trujillo, C.; Sánchez-Sanz, G., Interaction between Trinuclear Regium Complexes of Pyrazolate and Anions, a Computational Study. *International Journal of Molecular Sciences* **2020,** 21, 8036.
(10) Shur, V. B.; Tikhonova, I. A., Perfluorinated polymercuramacrocycles as anticrowns. Applications in catalysis. *Russ. Chem. Bull.* **2003,** 52, 2539-2554.
(11) Sartori, P.; Golloch, A., Darstellung und Eigenschaften von Tetrafluorphthalsäure-Derivaten. *Chem. Ber.* **1968,** 101, 2004-2009.
(12) Ball, M. C.; Brown, D. S.; Massey, A. G.; Wickens, D. A., A reinvestigation of o-phenylenemercurials: IV. Adducts of perfluorotribenzo[b,e,b][1,4,7]trimercuronin and the crystal and molecular structure of its 1 : 1 4-phenylpyridine solvate. *J. Organomet. Chem.* **1981,** 206, 265-277.
(13) Alvarez, S., A cartography of the van der Waals territories. *Dalton Trans.* **2013,** 42, 8617-8636.
(14) Tsunoda, M.; Gabbaï, F. P., μ6-η2:η2:η2:η2:η2:η2 As a New Bonding Mode for Benzene. *Journal of the American Chemical Society* **2000,** 122, 8335-8336.
(15) Haneline, M. R.; Tsunoda, M.; Gabbaï, F. P., π-Complexation of Biphenyl, Naphthalene, and Triphenylene to Trimeric Perfluoro-ortho-phenylene Mercury. Formation of Extended Binary Stacks with Unusual Luminescent Properties. *Journal of the American Chemical Society* **2002,** 124, 3737-3742.
(16) Filatov, A. S.; Greene, A. K.; Jackson, E. A.; Scott, L. T.; Petrukhina, M. A., Molecular curvature tradeoffs: Bending a planar trimercury unit over bowl-shaped polyaromatic hydrocarbons. *J. Organomet. Chem.* **2011,** 696, 2877-2881.

(17) Shubina, E. S.; Tikhonova, I. A.; Bakhmutova, E. V.; Dolgushin, F. M.; Antipin, M. Y.; Bakhmutov, V. I.; Sivaev, I. B.; Teplitskaya, L. N.; Chizhevsky, I. T.; Pisareva, I. V.; Bregadze, V. I.; Epstein, L. M.; Shur, V. B., Crown Compounds for Anions: Sandwich and Half-Sandwich Complexes of Cyclic Trimeric Perfluoro-o-phenylenemercury with Polyhedral closo-[B10H10]2− and closo-[B12H12]2− Anions. *Chemistry – A European Journal* **2001,** 7, 3783-3790.
(18) Tikhonova, I. A.; Dolgushin, F. M.; Tugashov, K. I.; Petrovskii, P. V.; Furin, G. G.; Shur, V. B., Coordination chemistry of polymercuramacrocycles. Complexation of cyclic trimeric perfluoro-o-phenylenemercury with neutral oxygeneous Lewis bases. *J. Organomet. Chem.* **2002,** 654, 123-131.
(19) Tsunoda, M.; Gabbaï, F. P., Complexation of methylparathion and bis(2-hydroxyethyl)sulfide by the tridentate lewis acid [(o-C6F4Hg)3]. *Heteroat. Chem* **2005,** 16, 292-297.
(20) Haneline, M. R.; Gabbaï, F. P., Electrophilic Double-Sandwiches Formed by Interaction of [Cp2Fe] and [Cp2Ni] with the Tridentate Lewis Acid [(o-C6F4Hg)3]. *Angew. Chem. Int. Ed.* **2004,** 43, 5471-5474.
(21) Tugashov, K. I.; Gribanyov, D. A.; Dolgushin, F. M.; Smol'yakov, A. F.; Peregudov, A. S.; Minacheva, M. K.; Strunin, B. N.; Tikhonova, I. A.; Shur, V. B., Coordination chemistry of mercury-containing anticrowns. Complexation of nitrate and sulfate anions with the three-mercury anticrown (o-C6F4Hg)3 and the influence of the nature of a countercation on the structure of the resulting nitrate complexes. *J. Organomet. Chem.* **2013,** 747, 167-173.
(22) Tikhonova, I. A.; Tugashov, K. I.; Dolgushin, F. M.; Yakovenko, A. A.; Petrovskii, P. V.; Furin, G. G.; Zaraisky, A. P.; Shur, V. B., Coordination chemistry of anticrowns: Complexation of cyclic trimeric perfluoro-o-phenylenemercury with nitro compounds. *J. Organomet. Chem.* **2007,** 692, 953-962.
(23) Tsunoda, M.; Gabbaï, F. P., Hexacoordination of a Dimethyl Sulfide Molecule. *Journal of the American Chemical Society* **2003,** 125, 10492-10493.
(24) Haneline, M. R.; Gabbaï, F. P., TTF and TCNQ adducts of trimeric perfluoro-ortho-phenylene mercury. *Comptes Rendus Chimie* **2004,** 7, 871-876.
(25) Fleischmann, M.; Jones, J. S.; Gabbaï, F. P.; Scheer, M., A comparative study of the coordination behavior of cyclo-P5 and cyclo-As5 ligand complexes towards the trinuclear Lewis acid complex (perfluoro-ortho-phenylene)mercury. *Chemical Science* **2015,** 6, 132-139.
(26) Taylor, T. J.; Gabbaï, F. P., Supramolecular Stabilization of α,ω-Diphenylpolyynes by Complexation to the Tridentate Lewis Acid [o-C6F4Hg]3. *Organometallics* **2006,** 25, 2143-2147.
(27) King, J. B.; Tsunoda, M.; Gabbaï, F. P., Complexation of Aldehydes and Ketones by Trimeric Perfluoro-ortho-phenylene Mercury, a Tridentate Lewis Acid. *Organometallics* **2002,** 21, 4201-4205.
(28) Tugashov, K. I.; Gribanyov, D. A.; Dolgushin, F. M.; Smol'yakov, A. F.; Peregudov, A. S.; Klemenkova, Z. S.; Barakovskaya, I. G.; Tikhonova, I. A.; Shur, V. B., Coordination Chemistry of Anticrowns. Interaction of the Perfluorinated Three-Mercury Anticrown (o-C6F4Hg)3 with Azacrowns. *Organometallics* **2019,** 38, 2910-2918.
(29) Tugashov, K. I.; Gribanyov, D. A.; Dolgushin, F. M.; Smol'yakov, A. F.; Peregudov, A. S.; Minacheva, M. K.; Tikhonova, I. A.; Shur, V. B., Coordination Chemistry of Anticrowns. Synthesis and Structures of Double-Decker Sandwich Complexes of the Three-Mercury Anticrown (o-C6F4Hg)3 with Halide Anions

Containing and Not Containing Coordinated Dibromomethane Molecules. *Organometallics* **2016,** 35, 2197-2206.
(30) Gil, D. M.; Echeverría, J.; Alvarez, S., Tetramethylammonium Cation: Directionality and Covalency in Its Interactions with Halide Ions. *Inorg. Chem.* **2022**.
(31) Tikhonova, I. A.; Gribanyov, D. A.; Tugashov, K. I.; Dolgushin, F. M.; Smol'yakov, A. F.; Peregudov, A. S.; Klemenkova, Z. S.; Shur, V. B., Coordination chemistry of mercury-containing anticrowns. Self-assembly of unusual supramolecular aggregates in the interaction of the three-mercury anticrown with crown ethers in the presence of neutral monodentate oxygenous Lewis bases. *ARKIVOC* **2011,** 2011, 172-184.
(32) Tikhonova, I. A.; Dolgushin, F. M.; Yanovsky, A. I.; Starikova, Z. A.; Petrovskii, P. V.; Furin, G. G.; Shur, V. B., Complexation of cyclic trimeric perfluoro-o-phenylenemercury with nitriles. A remarkable sensitivity of the composition and structure of the resulting complexes to the nature of a nitrile. *J. Organomet. Chem.* **2000,** 613, 60-67.
(33) Echeverría, J.; Velásquez, J. D.; Alvarez, S., Understanding the Interplay of Dispersion, Charge Transfer, and Electrostatics in Noncovalent Interactions: The Case of Bromine–Carbonyl Short Contacts. *Cryst. Growth Des.* **2020,** 20, 7180-7187.
(34) Varadwaj, A.; Varadwaj, P. R.; Yamashita, K., Do surfaces of positive electrostatic potential on different halogen derivatives in molecules attract? like attracting like! *J. Comput. Chem.* **2018,** 39, 343-350.
(35) Zierkiewicz, W.; Michalczyk, M.; Maris, T.; Wysokiński, R.; Scheiner, S., Experimental and theoretical evidence of attractive interactions between dianions: [PdCl4]2−···[PdCl4]2−. *Chem. Commun.* **2021,** 57, 13305-13308.
(36) Weinhold, F., Anti-Electrostatic Pi-Hole Bonding: How Covalency Conquers Coulombics. *Molecules* **2022,** 27, 377.
(37) Grdenić, D., The structural chemistry of mercury. *Quarterly Reviews, Chemical Society* **1965,** 19, 303-328.
(38) Kaupp, M.; von Schnering, H. G., Ab Initio Comparison of the (MX2)2 Dimers (M = Zn, Cd, Hg; X = F, Cl, H) and Study of Relativistic Effects in Crystalline HgF2. *Inorg. Chem.* **1994,** 33, 4718-4722.
(39) Kaupp, M.; von Schnering, H. G., Dominance of Linear 2-Coordination in Mercury Chemistry: Quasirelativistic and Nonrelativistic ab Initio Pseudopotential Study of (HgX2)2 (X = F, Cl, Br, I, H). *Inorg. Chem.* **1994,** 33, 2555-2564.
(40) Tikhonova, I. A.; Tugashov, K. I.; Dolgushin, F. M.; Korlyukov, A. A.; Petrovskii, P. V.; Klemenkova, Z. S.; Shur, V. B., Coordination chemistry of mercury-containing anticrowns. Synthesis and structures of the complexes of cyclic trimeric perfluoro-o-phenylenemercury with ethanol, THF and bis-2,2′-tetrahydrofuryl peroxide. *J. Organomet. Chem.* **2009,** 694, 2604-2610.
(41) Taylor, T. J.; Burress, C. N.; Gabbaï, F. P., Lewis Acidic Behavior of Fluorinated Organomercurials. *Organometallics* **2007,** 26, 5252-5263.
(42) Gomila, R. M.; Bauza, A.; Mooibroek, T. J.; Frontera, A., π-Hole spodium bonding in tri-coordinated Hg(ii) complexes. *Dalton Transactions* **2021,** 50, 7545-7553.
(43) Xia, T.; Li, D.; Cheng, L., Theoretical analysis of the spodium bonds in HgCl2···L (L = ClR, SR2, and PR3) dimers. *Chem. Phys.* **2020,** 539, 110978.
(44) Coulson, C. A., 276. The nature of the bonding in xenon fluorides and related molecules. *Journal of the Chemical Society (Resumed)* **1964**, 1442-1454.

(45) Landis, C. R.; Weinhold, F., 18-electron rule and the 3c/4e hyperbonding saturation limit. *J. Comput. Chem.* **2016,** 37, 237-241.
(46) Glendening, E. D.; Weinhold, F., Natural resonance theory: I. General formalism. *J. Comput. Chem.* **1998,** 19, 593-609.
(47) Glendening, E. D.; Weinhold, F., Natural resonance theory: II. Natural bond order and valency. *J. Comput. Chem.* **1998,** 19, 610-627.
(48) Landis, C. R.; Weinhold, F., Valence and extra-valence orbitals in main group and transition metal bonding. *J. Comput. Chem.* **2007,** 28, 198-203.
(49) Zhang, G.; Yue, H.; Weinhold, F.; Wang, H.; Li, H.; Chen, D., Resonance Character of Copper/Silver/Gold Bonding in Small Molecule···M□X (X=F, Cl, Br, CH3, CF3) Complexes. *ChemPhysChem* **2015,** 16, 2424-2431.
(50) Groom, C. R.; Bruno, I. J.; Lightfoot, M. P.; Ward, S. C., The Cambridge Structural Database. *Acta Crystallogr. Sect. B* **2016,** 72, 171-179.
(51) Gaussian 16, Revision B.01, Frisch, M. J.; Trucks, G. W.; Schlegel, H. B.; Scuseria, G. E.; Robb, M. A.; Cheeseman, J. R.; Scalmani, G.; Barone, V.; Petersson, G. A.; Nakatsuji, H.; Li, X.; Caricato, M.; Marenich, A. V.; Bloino, J.; Janesko, B. G.; Gomperts, R.; Mennucci, B.; Hratchian, H. P.; Ortiz, J. V.; Izmaylov, A. F.; Sonnenberg, J. L.; Williams-Young, D.; Ding, F.; Lipparini, F.; Egidi, F.; Goings, J.; Peng, B.; Petrone, A.; Henderson, T.; Ranasinghe, D.; Zakrzewski, V. G.; Gao, J.; Rega, N.; Zheng, G.; Liang, W.; Hada, M.; Ehara, M.; Toyota, K.; Fukuda, R.; Hasegawa, J.; Ishida, M.; Nakajima, T.; Honda, Y.; Kitao, O.; Nakai, H.; Vreven, T.; Throssell, K.; Montgomery, J. A., Jr.; Peralta, J. E.; Ogliaro, F.; Bearpark, M. J.; Heyd, J. J.; Brothers, E. N.; Kudin, K. N.; Staroverov, V. N.; Keith, T. A.; Kobayashi, R.; Normand, J.; Raghavachari, K.; Rendell, A. P.; Burant, J. C.; Iyengar, S. S.; Tomasi, J.; Cossi, M.; Millam, J. M.; Klene, M.; Adamo, C.; Cammi, R.; Ochterski, J. W.; Martin, R. L.; Morokuma, K.; Farkas, O.; Foresman, J. B.; Fox, D. J. Gaussian, Inc., Wallingford CT, 2016.
(52) Echeverría, J.; Cirera, J.; Alvarez, S., Mercurophilic interactions: a theoretical study on the importance of ligands. *Phys. Chem. Chem. Phys.* **2017,** 19, 11645-11654.
(53) Mentel, Ł. M.; Baerends, E. J., Can the Counterpoise Correction for Basis Set Superposition Effect Be Justified? *Journal of Chemical Theory and Computation* **2014,** 10, 252-267.
(54) *GaussView, version 5, R. Dennington, T. Keith and J. Millam, Semichem Inc., Shawnee Mission, KS, 2009.* . ed.
(55) Shao, Y.; Gan, Z.; Epifanovsky, E.; Gilbert, A. T. B.; Wormit, M.; Kussmann, J.; Lange, A. W.; Behn, A.; Deng, J.; Feng, X.; Ghosh, D.; Goldey, M.; Horn, P. R.; Jacobson, L. D.; Kaliman, I.; Khaliullin, R. Z.; Kuś, T.; Landau, A.; Liu, J.; Proynov, E. I.; Rhee, Y. M.; Richard, R. M.; Rohrdanz, M. A.; Steele, R. P.; Sundstrom, E. J.; Woodcock, H. L.; Zimmerman, P. M.; Zuev, D.; Albrecht, B.; Alguire, E.; Austin, B.; Beran, G. J. O.; Bernard, Y. A.; Berquist, E.; Brandhorst, K.; Bravaya, K. B.; Brown, S. T.; Casanova, D.; Chang, C.-M.; Chen, Y.; Chien, S. H.; Closser, K. D.; Crittenden, D. L.; Diedenhofen, M.; DiStasio, R. A.; Do, H.; Dutoi, A. D.; Edgar, R. G.; Fatehi, S.; Fusti-Molnar, L.; Ghysels, A.; Golubeva-Zadorozhnaya, A.; Gomes, J.; Hanson-Heine, M. W. D.; Harbach, P. H. P.; Hauser, A. W.; Hohenstein, E. G.; Holden, Z. C.; Jagau, T.-C.; Ji, H.; Kaduk, B.; Khistyaev, K.; Kim, J.; Kim, J.; King, R. A.; Klunzinger, P.; Kosenkov, D.; Kowalczyk, T.; Krauter, C. M.; Lao, K. U.; Laurent, A. D.; Lawler, K. V.; Levchenko, S. V.; Lin, C. Y.; Liu, F.; Livshits, E.; Lochan, R. C.; Luenser, A.; Manohar, P.; Manzer, S. F.; Mao, S.-P.; Mardirossian, N.; Marenich, A. V.; Maurer, S. A.; Mayhall, N. J.; Neuscamman, E.; Oana, C. M.; Olivares-Amaya, R.; O'Neill, D. P.; Parkhill, J. A.; Perrine, T. M.; Peverati, R.; Prociuk, A.; Rehn, D. R.; Rosta, E.; Russ, N. J.; Sharada, S. M.; Sharma, S.; Small, D. W.; Sodt, A.; Stein, T.;

Stück, D.; Su, Y.-C.; Thom, A. J. W.; Tsuchimochi, T.; Vanovschi, V.; Vogt, L.; Vydrov, O.; Wang, T.; Watson, M. A.; Wenzel, J.; White, A.; Williams, C. F.; Yang, J.; Yeganeh, S.; Yost, S. R.; You, Z.-Q.; Zhang, I. Y.; Zhang, X.; Zhao, Y.; Brooks, B. R.; Chan, G. K. L.; Chipman, D. M.; Cramer, C. J.; Goddard, W. A.; Gordon, M. S.; Hehre, W. J.; Klamt, A.; Schaefer, H. F.; Schmidt, M. W.; Sherrill, C. D.; Truhlar, D. G.; Warshel, A.; Xu, X.; Aspuru-Guzik, A.; Baer, R.; Bell, A. T.; Besley, N. A.; Chai, J.-D.; Dreuw, A.; Dunietz, B. D.; Furlani, T. R.; Gwaltney, S. R.; Hsu, C.-P.; Jung, Y.; Kong, J.; Lambrecht, D. S.; Liang, W.; Ochsenfeld, C.; Rassolov, V. A.; Slipchenko, L. V.; Subotnik, J. E.; Van Voorhis, T.; Herbert, J. M.; Krylov, A. I.; Gill, P. M. W.; Head-Gordon, M., Advances in molecular quantum chemistry contained in the Q-Chem 4 program package. *Mol. Phys.* **2015,** 113, 184-215.

(56) *NBO 7.0. E. D. Glendening, J, K. Badenhoop, A. E. Reed, J. E. Carpenter, J. A. Bohmann, C. M. Morales, P. Karafiloglou, C. R. Landis, and F. Weinhold, Theoretical Chemistry Institute, University of Wisconsin, Madison (2018).* ed.

For Table of Contents Only

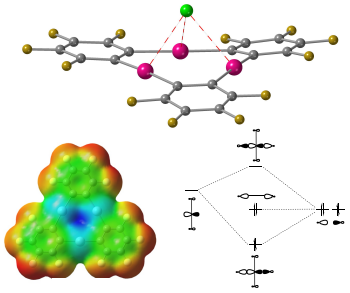

Hg_3-anticrowns are capable to bind a wide range of Lewis bases, both anionic and neutral, via their three metal centers, where not only electrostatics but also the orbitals involved in the interaction determine the final geometry and stability of the adducts. Moreover, molecular orbital theory allows the rationalization of the formation of a pseudo-octahedral second coordination sphere in d^{10} closed-shell linear complexes.